Zeitschrift: IABSE publications = Mémoires AIPC = IVBH Abhandlungen
Band: 30 (1970)

Artikel: Deformation capacity of steel plate elements
Autor: Kato, Ben / Aoki, Hirofumi
DOI: https://doi.org/10.5169/seals-23580

Nutzungsbedingungen
Die ETH-Bibliothek ist die Anbieterin der digitalisierten Zeitschriften auf E-Periodica. Sie besitzt keine Urheberrechte an den Zeitschriften und ist nicht verantwortlich für deren Inhalte. Die Rechte liegen in der Regel bei den Herausgebern beziehungsweise den externen Rechteinhabern. Das Veröffentlichen von Bildern in Print- und Online-Publikationen sowie auf Social Media-Kanälen oder Webseiten ist nur mit vorheriger Genehmigung der Rechteinhaber erlaubt. Mehr erfahren

Conditions d'utilisation
L'ETH Library est le fournisseur des revues numérisées. Elle ne détient aucun droit d'auteur sur les revues et n'est pas responsable de leur contenu. En règle générale, les droits sont détenus par les éditeurs ou les détenteurs de droits externes. La reproduction d'images dans des publications imprimées ou en ligne ainsi que sur des canaux de médias sociaux ou des sites web n'est autorisée qu'avec l'accord préalable des détenteurs des droits. En savoir plus

Terms of use
The ETH Library is the provider of the digitised journals. It does not own any copyrights to the journals and is not responsible for their content. The rights usually lie with the publishers or the external rights holders. Publishing images in print and online publications, as well as on social media channels or websites, is only permitted with the prior consent of the rights holders. Find out more

Download PDF: 02.02.2026

ETH-Bibliothek Zürich, E-Periodica, https://www.e-periodica.ch

Deformation Capacity of Steel Plate Elements

Aptitude à la déformation des plaques d'acier

Verformungsfähigkeit von Stahlplattenelementen

BEN KATO
Professor, Faculty of Engineering, University of Tokyo, Tokyo, Japan

HIROFUMI AOKI
Graduate Student, University of Tokyo, Tokyo, Japan

Introduction

The stress-strain relation of the structural steel is characterized by the long plastic flow started from the yield point and followed by the strain hardening. When the steel bar of the uniform section is subject to a tensile load, its load-deformation diagram will present the similar behavior as that of the stress-strain diagram, and it seems to have enough ductility.

This behavior will become somewhat different when the stress in the section changes continuously along the length of the bar. Consider the model shown in Fig. 1, where the cross section of the bar changes continuously and the section A–A has the minimum cross sectional area. The yield will firstly occur at the section A–A when the bar is subject to a tensile load, and without the further increase of the applied load, the vicinity of the section A–A will never yield because the strain at the section A–A remains in the plastic flow range. This means that, in such a specimen, the plastic flow will not appear without the further increase of the applied load as the yield section A–A has geometrically zero length. When the strain at the section A–A enters into the strain hardening range, the applied load will increase correspondingly, and the yielded zone will extend to the vicinity of the section A–A.

The maximum strength and the maximum deformation*) of the specimen will be reached when the stress at the section A–A reaches the tensile strength of the material. Thus the inelastic deformation capacity will depend upon the

*) In this paper, the maximum deformation means the deformation of the specimen at the maximum strength state, not the deformation at the breaking of the specimen.

yield ratio of the material (the ratio of the yield point to the tensile strength of the material).

If, for instance, there would be a material having the yield ratio which equals unity, the material of elastic-perfectly plastic, the specimen will break up abruptly as soon as the stress in the section A–A reaches the yield point, and no plastic deformation may be observed.

The similar phenomenon may be observed when the member is prismatic, however the stress changes along its length. This is approximately the case of the flanges of wide-flange beams having the moment gradient, then in this case, the rotation capacity of the beam may be controlled by the yield ratio of the material, such as LAY had implied [1].

The idea described above will be verified by the following analysis and experiments.

The Case of Gradual Stress Change — Stress Concentration is Negligible

A steel specimen having the uniform thickness is subject to a tensile load in the direction of the x-axis as shown in Fig. 1. The specimen is assumed to be symmetric about both x and y axis. The change of the sectional area along the length of the specimen is assumed to be so gradual as to be able to neglect the effect of the stress concentration.

The stress-strain relation of the material is simplified by four straight lines as shown in Fig. 2.

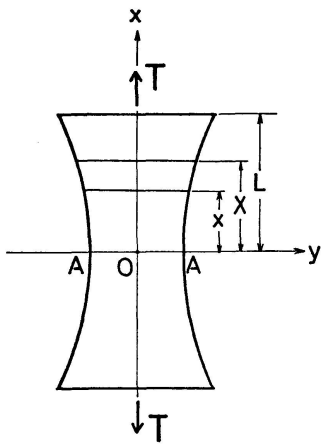

Fig. 1.

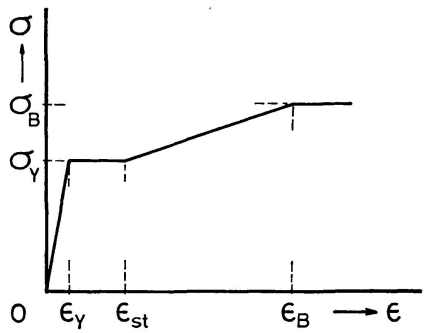

Fig. 2.

where,

σ_Y: yield point,
σ_B: tensile strength,
ϵ_Y: strain at yield point,
ϵ_{st}: strain at the start of strain hardening,
ϵ_B: strain at tensile strength point.

The maximum tensile strength of the specimen is reached when the stress in the minimum section of the specimen attains to σ_B.

$$T_{max} = \sigma_B A(0), \tag{1}$$

where, T_{max}: maximum tensile strength of the specimen,
$A(0)$: minimum sectional area of the specimen.

The average tensile stress at an arbitrary section of the specimen when subject to the tensile load having the magnitude of $\alpha T_{max} (0 \leqq \alpha \leqq 1.0)$ is expressed as,

$$\sigma(x) = \frac{\alpha T_{max}}{A(x)} = \alpha \sigma_B \frac{A(0)}{A(x)}, \tag{2}$$

where, $\sigma(x)$: average stress at x,
$A(x)$: sectional area at x.

The extension of the yielded zone X is obtained by introducing σ_Y to $\sigma(x)$ of eq. (2),

$$\sigma_Y = \alpha \sigma_B \frac{A(0)}{A(X)}.$$

The alternative expression of the above equation is as follows, introducing the symbol $Y = \sigma_Y/\sigma_B$; the yield ratio of the material,

$$A(X) - \frac{\alpha}{Y} A(0) = 0. \tag{3}$$

Eq. (3) gives the extension of the yielded zone X under the given load αT_{max}, and it may be seen from this equation that, in case of elastic-perfectly plastic material ($Y = 1$), $A(X)$ is at most equal to $A(0)$ even in the maximum strength state ($\alpha = 1$), and this means that no plastic deformation of the specimen may be expected.

The elongation of the half length of the specimen δ_L, when the tensile load be $T = \alpha T_{max}$ and the extension of the yielded zone be X, is given by,

$$\delta_L = X \epsilon_{st} + \frac{\epsilon_B - \epsilon_{st}}{1-Y} \int_0^X \left[\alpha \frac{A(0)}{A(x)} - Y \right] dx + \frac{\alpha \epsilon_Y}{Y} \int_X^L \frac{A(0)}{A(x)} dx. \tag{4}$$

The elongation δ_{max} at the maximum load is obtained by introducing $\alpha = 1$ into eq. (4),

$$\delta_{max} = \left[\epsilon_{st} - \frac{Y}{1-Y} (\epsilon_B - \epsilon_{st}) \right] X + \frac{\epsilon_B - \epsilon_{st}}{1-Y} \int_0^X \frac{A(0)}{A(x)} dx + \frac{\epsilon_Y}{Y} \int_X^L \frac{A(0)}{A(x)} dx, \tag{5}$$

$$A(X) - \frac{1}{Y} A(0) = 0.$$

Fig. 3 is the schematical illustration of eq. (5), assuming, for the simplicity, that ϵ_{st} and ϵ_B have the same values for various grades of steel. The larger the yield ratio of the material, the smaller the deformation capacity, though the

descending paths become somewhat different on accordance with the shape of the specimen.

To verify the theoretical prediction above described, experiments were conducted using various grades of steel. The shape of the test specimens is as shown in Fig. 4. The elongation of the specimens between points G and G' were measured by dial gauges as shown in Fig. 4 for each step of loading.

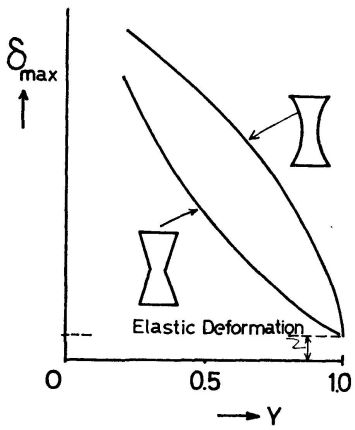

Fig. 3.

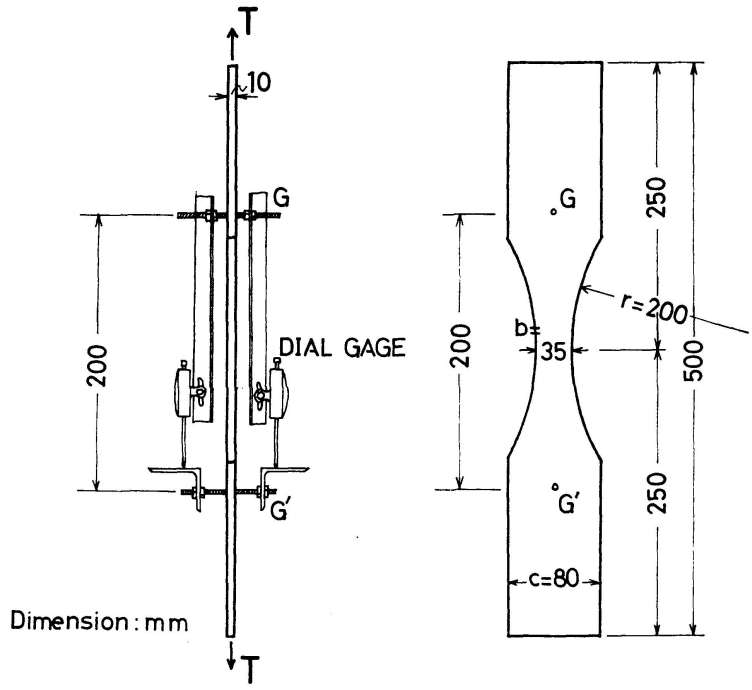

Fig. 4.

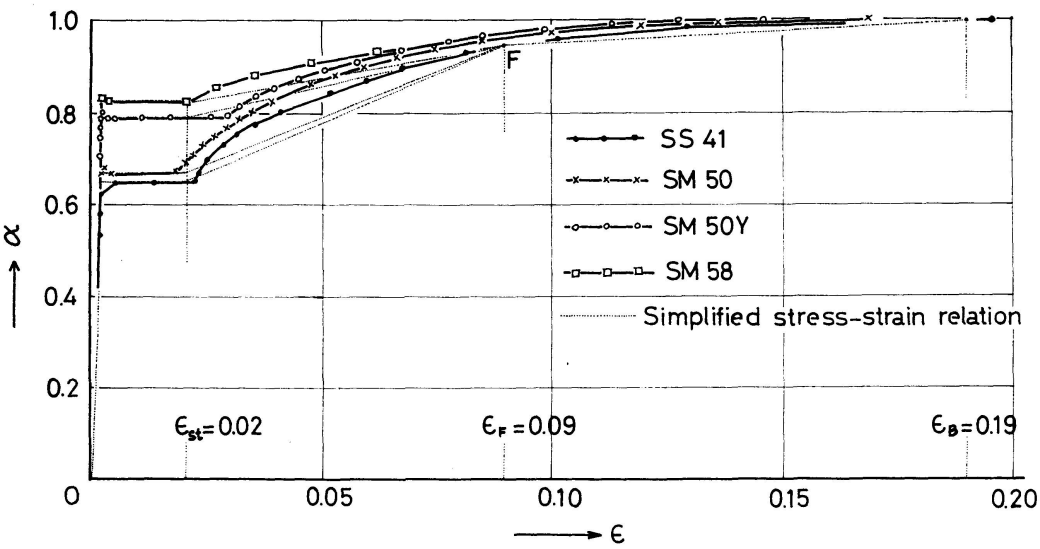

Fig. 5.

The stress-strain diagrams of materials used are shown in Fig. 5, and their specific values are shown in Table 1. The simplification of the stress-strain diagram for the use of calculation was made as follows:

Table 1. Mechanical Properties of Various Grades of Steel

Grade of steel	Young's modulus E	Yield point σ_Y	Tensile strength σ_B	Yield ratio of material $Y=\sigma_Y/\sigma_B$	Strain at the strain hardening point ϵ_{st}	Strain at the tensile strength point ϵ_B
	in tons per square centimetre					
SS41	2005	3.03	4.62	0.655	0.022	0.195
SM50	2095	3.85	5.76	0.669	0.019	0.177
SM50Y	2090	4.37	5.51	0.793	0.031	0.163
SM58	2065	5.01	6.05	0.827	0.020	0.135

a) ϵ_{st} and ϵ_B are assumed to be 0.02, 0.19 respectively for all grades of steel here, for simplicity.

b) It is difficult to determine ϵ_B exactly because the unlimited flow occurs at the vicinity of this point, so the point, $F\,(\alpha = \sigma/\sigma_B = 0.95,\ \epsilon_F = 0.09)$ was chosen as the first point to be checked.

The simplified stress-strain diagrams were thus constructed by connecting these points with straight lines as shown in Fig. 5.

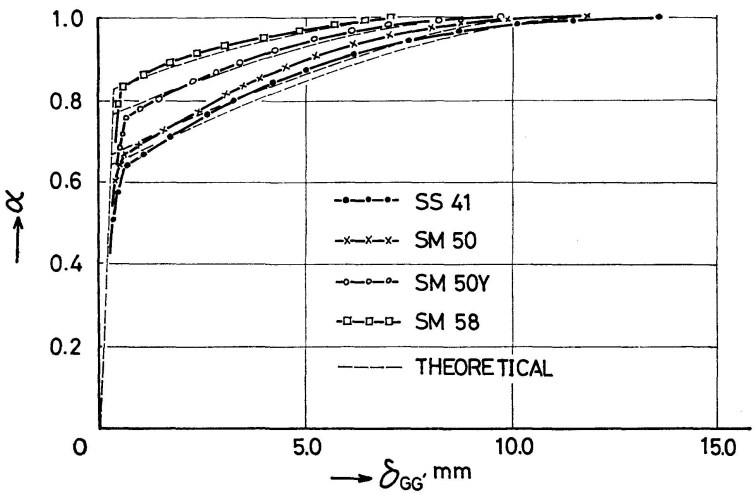

Fig. 6.

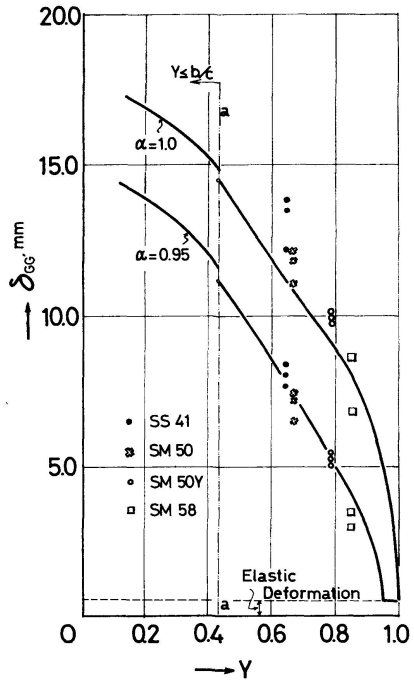

Fig. 7.

The diagrams for the load index α versus elongation for various grades of steel obtained from the experiments are plotted in Fig. 6, where theoretical predictions based on the simplified stress-strain diagrams now obtained are also shown in broken lines.

The relation between the maximum elongation and the yield ratio of the material is shown in Fig. 7. At the loading state $\alpha = 0.95$, the theoretical

prediction and the experimental results are in good accordance, at the ultimate state ($\alpha = 1$), however, the experimental results exhibit some scattering, which perhaps be resulted from the difficulty of measuring ϵ_B exactly as mentioned before. The left side of the dotted line a–a in this figure shows the domain where the parallel parts of the specimen yields perfectly, and the longer the parallel parts, the larger the jump of elongation at the a–a line.

The Case of Steep Stress Change — Stress Concentration must be Considered

As the typical example of the case of stress concentration, the plate with a round hole as shown in Fig. 8 was adopted, and the behavior was investigated until its ultimate state theoretically and experimentally.

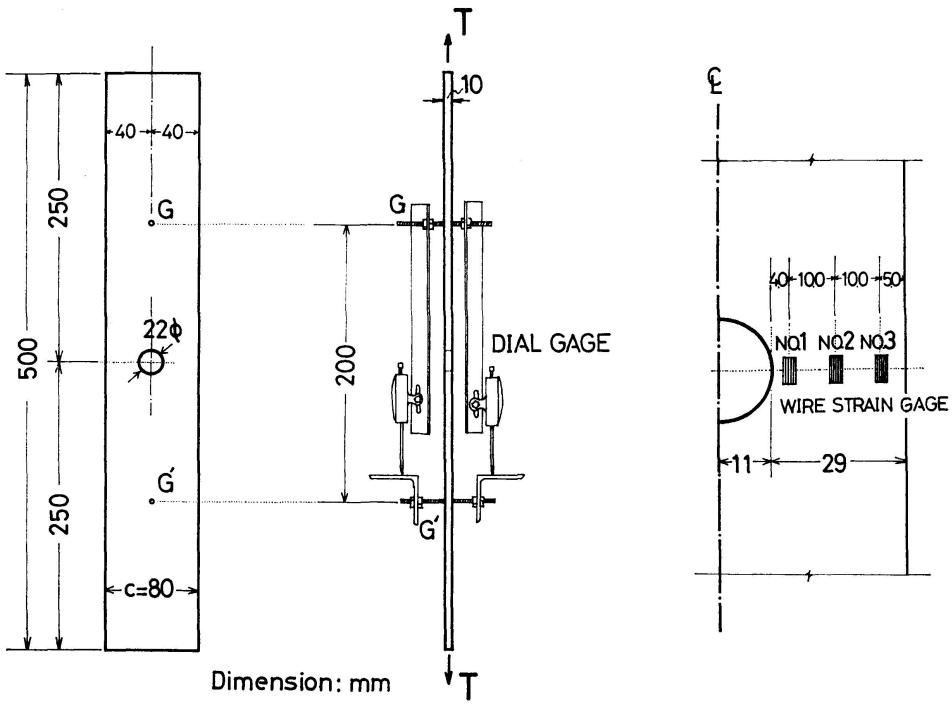

Fig. 8.

In order to investigate the effect of the yield ratio of the material, the specimens of various grades of steel were examined also in this case.

The rigorous theoretical solution of such a plate in elastic-plastic range has not yet been obtained, so the numerical analysis by the finite element method extended to the elastic-plastic range on the basis of the plastic flow theory [2] is performed in this paper. The specimen is divided into triangular elements shown in Fig. 9, considering the symmetry of the specimen and the available capacity of the computer.

The detailed description of the finite element technique adopted here is shown in Appendix I, and the behavior of this specimen obtained by the calcu-

lation and the experiment is illustrated bellow rather minutely taking the case of SM 50 steel (equivalent to ST-52) as an example.

The relation between the true stress and the natural strain must be used in this case because the material be in biaxial state of stress in the vicinity of the hole, and this is shown in Fig. 10, which is obtained from the tensile specimen test, the conventional stress-strain diagram is also shown in this figure for comparison.

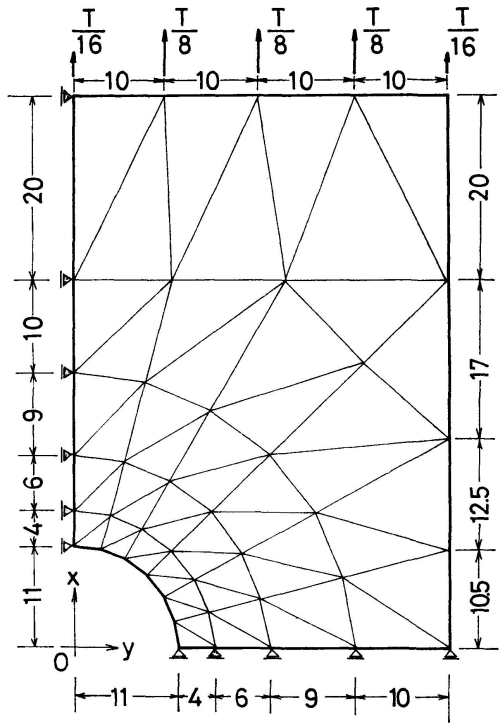

Dimension: mm

Fig. 9.

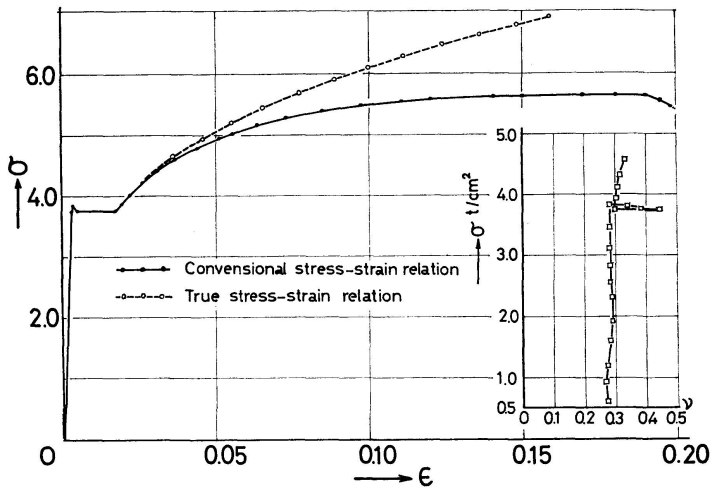

Fig. 10.

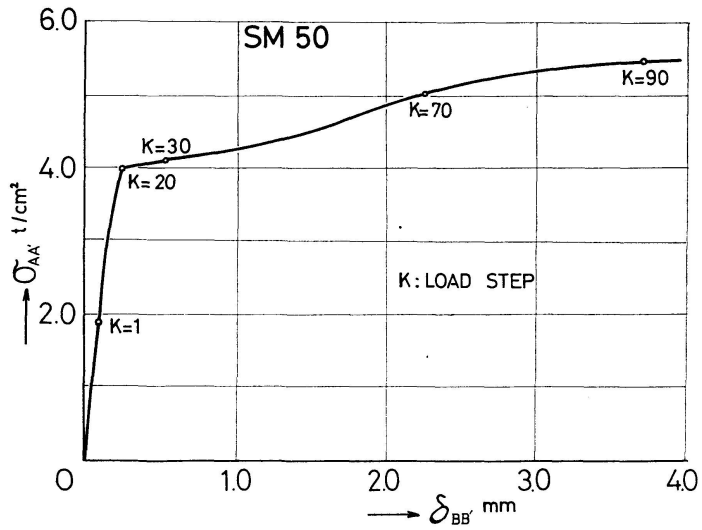

Fig. 11.

The theoretical relation for the mean stress at the minimum section A–A' versus the elongation of the specimen between B–B' is shown in Fig. 11. The theoretical overall yielding of this specimen had occured at the mean stress

4.0 ton/cm² in the section A–A', whereas the yield point of this material was 3.85 ton/cm² as was seen in Fig. 10, this difference was caused by having been assumed VON MISES' yield condition in this analysis.

The spread of the yielded zone and the distribution of stress and strain along the section A–A' are shown in Fig. 12 for various load steps K which correspond to the same symbol shown in Fig. 11. The meaning of other symbols used in this figure is as follows,

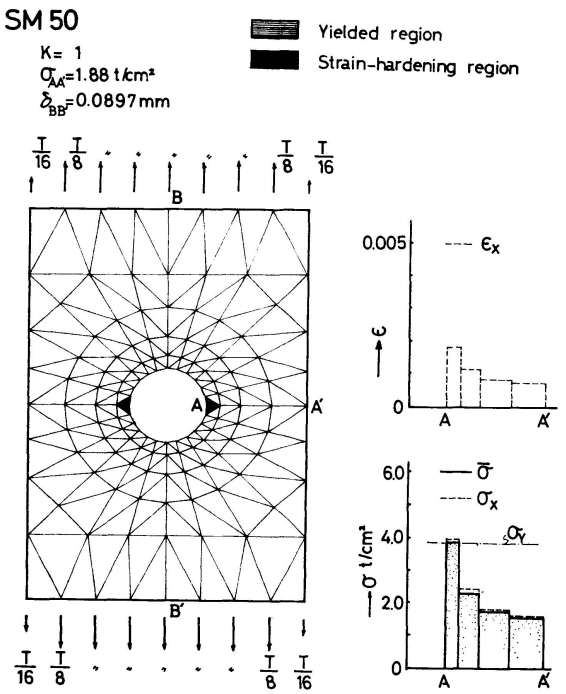

Fig. 12-1.

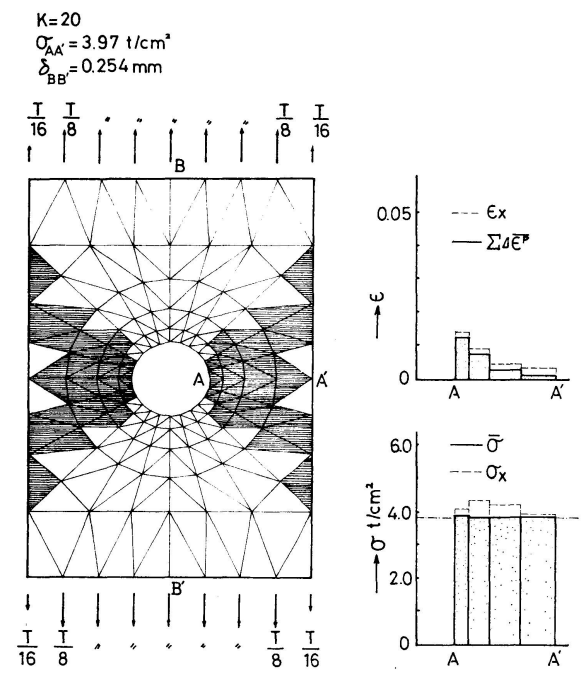

Fig. 12-2.

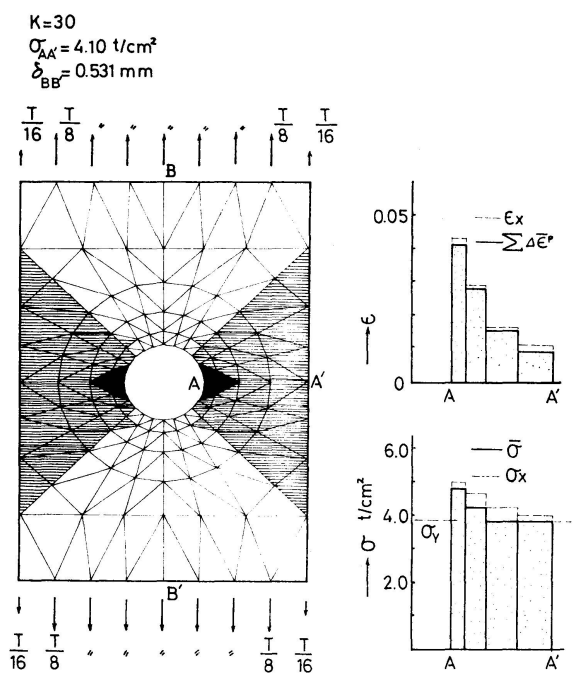

Fig. 12-3.

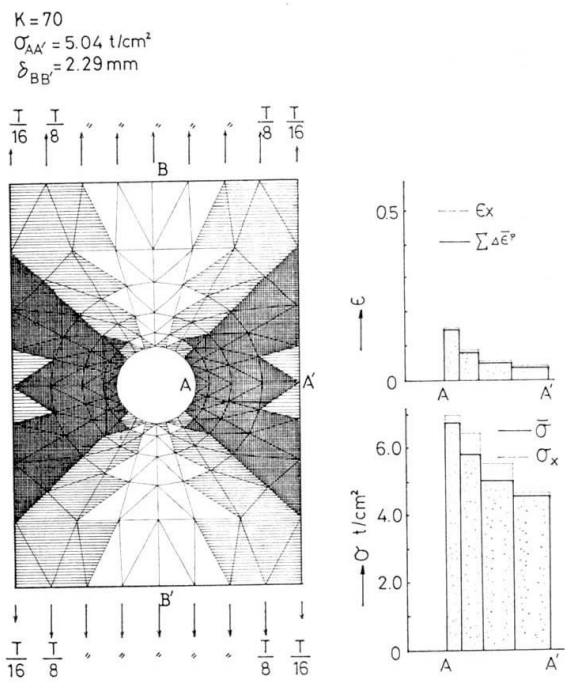

Fig. 12-4.

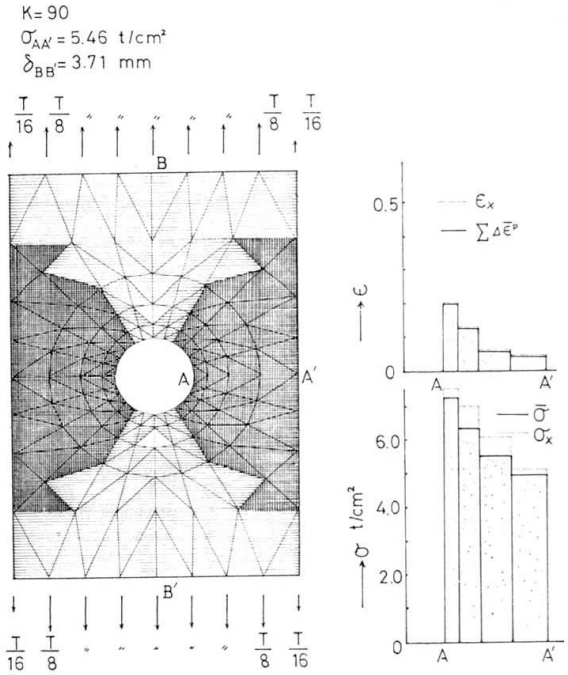

Fig. 12-5.

$\sum \Delta \bar{\epsilon}^p$: plastic strain according to the definition of the plastic flow theory.

$\bar{\sigma} = \sqrt{\sigma_x^2 + \sigma_y^2 - \sigma_x \sigma_y + 3\tau^2}$: equivalent stress.

Measured strains at the locations of No. 1–No. 3 shown in Fig. 8 are compared with the calculated strains in Fig. 13. In the finite element method, the strain is assumed to distribute uniformly in each triangular element, while the actual strain will change continuously in the whole region, so the average of the strains at neighbouring triangular elements is considered to be the equivalent strain which should be compared with measured strain. The average strain $\bar{\epsilon}$ was calculated by the following equation,

$$\bar{\epsilon} = \frac{1}{V_i + V_{i+1}} (\epsilon_i V_i + \epsilon_{i+1} V_{i+1}),$$

where V_1, V_{i+1} are volumes of neighbouring triangular elements and ϵ_i, ϵ_{i+1} are calculated strains at respective elements as illustrated in Fig. 14.

The diagram for mean stress at the minimum section A–A' versus elongation of the specimen between points G and G' is compared with the test results in Fig. 15.

The agreement seems to be satisfactory for the both cases.

As the final step, the relation between the deformation capacity of such specimens and the yield ratios of the material used is investigated. In order to see the results on a common base, ϵ_{st} and ϵ_B were assueed to have the identical values for various grades of steel as was done in the previous section. In this

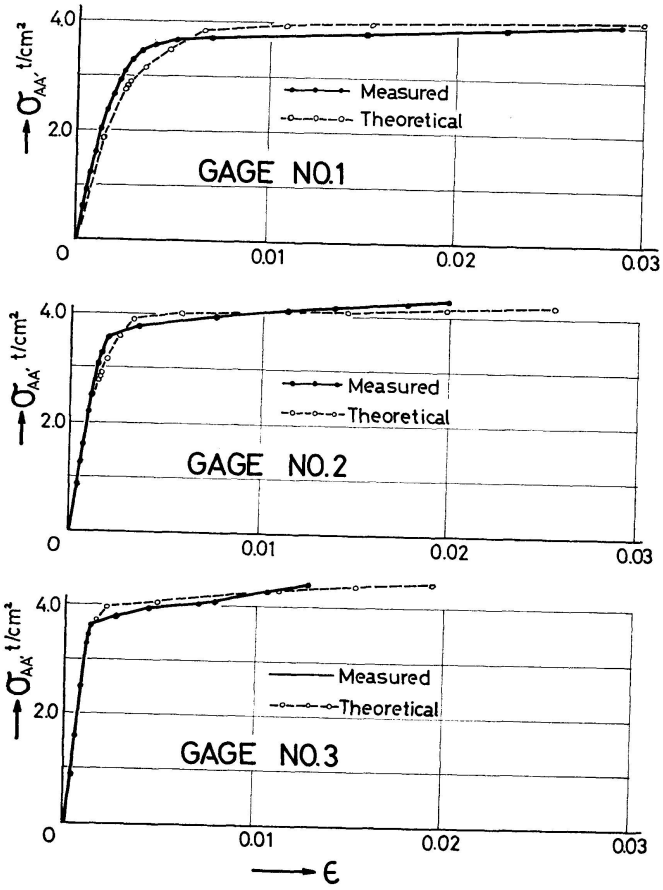

Fig. 13.

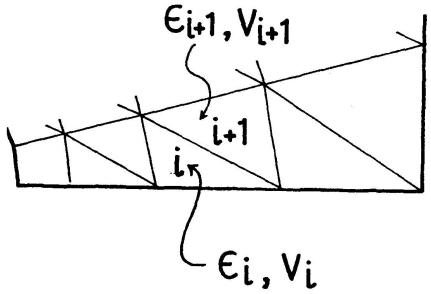

Fig. 14.

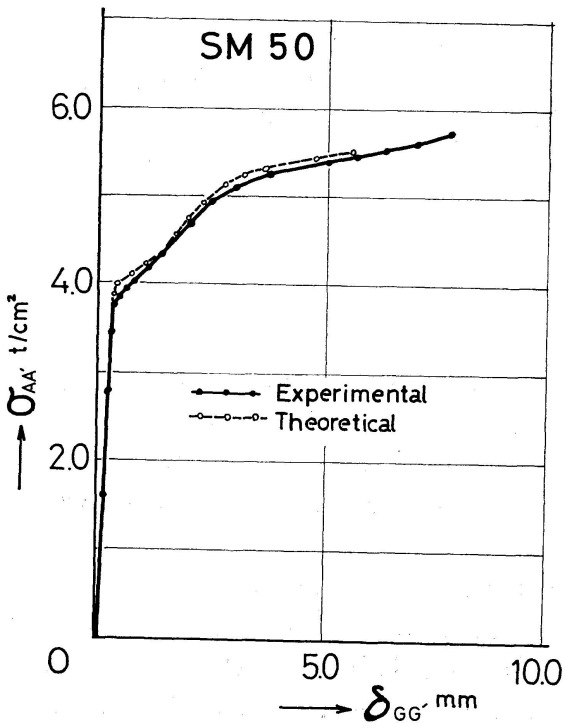

Fig. 15.

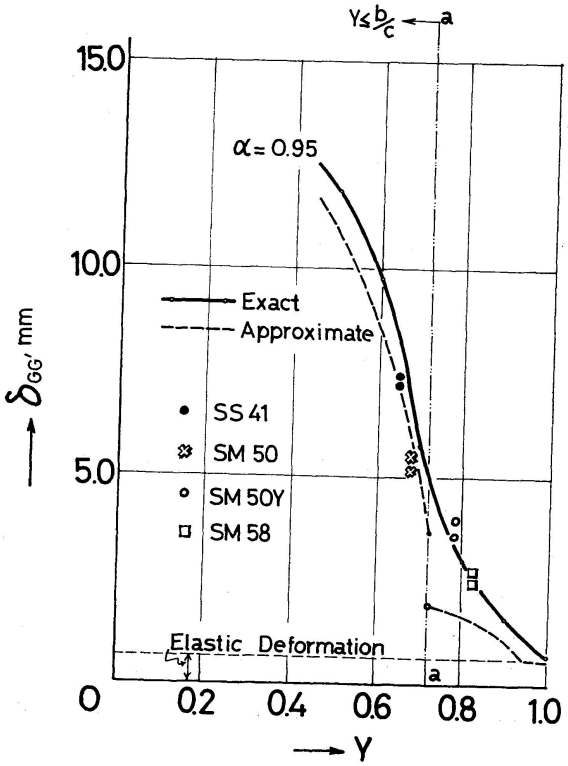

Fig. 16.

type of the specimen, the rupture occurs suddenly when the load reaches the maximum without showing any necking at the part of the minimum section, and it is very difficult to measure the elongation at the maximum load point, so both theoretical and experimental values are compared at the loading level $\alpha = T/T_{max} = 0.95$ in this study. The solid line of Fig. 16 shows the theoretical relation between the elongation and the yield ratio of the material. Test results of specimens having various values of yield ratios are plotted in this figure. Mechanical properties of all steels indicated in the figure have been shown in Table 1. The figure shown by a broken line is the prediction based on the simple theory described in the previous section which neglects the effect of stress concentration. The left side of the dotted line a–a in this figure shows the domain where the whole section of no hole yields thoroughly. It can be seen that the deformation capacity increases drastically when the yield ratio of the material is smaller than the value shown by this dotted line.

Conclusion

It has been shown theoretically and experimentally that the elongation capacity of the steel plates of which sectional area change along their length was controled by the yield ratio of the material used. The larger the value of the yield ratio, the smaller the elongation capacity of the member.

It may be said from this point of view that it should be careful when the high yield strength steel be used in a tension member bolted or rivetted at its connections or in tapered or notched shape, because the high yield strength steel generally has the high yield ratio.

It has also been shown that the elongation capacity increases drastically when the whole section of the parallel part of the member could yield thoroughly before the maximum strength of the specimen be reached. It may be safe to assume that the maximum average stress in the minimum section at the maximum strength state of the specimen is at least equal to the tensile strength of the material σ_B even in the case of the stess concentration be severe, then the condition above mentioned may be written as,

$$A_{min}\,\sigma_B \geqq A_p\,\sigma_Y\,, \quad \text{or} \quad A_{min} \geqq Y\,A_p\,,$$

where A_{min}: the minimum sectional area of the member,

A_p: the sectional area of the parallel part.

This means that the minimum area should be larger than Y times the area of the parallel part. For the practical purpose, the above criterion may be useful to secure the enough ductility of the steel tension member.

Appendix I. Extension of the Finite Element Method for Plane Stress Analysis to the Inelastic Range

The material dealt in this procedure is an isotropic and ductile one obeying the VON MISES yield condition, and the PRANDTL-REUSS' loading function.

Based on the incremental strain theory, the deformations predicted for the volume element will be different for each loading path, then the boundary of elastic and plastic region should be determined by giving the load increments. And the stiffness matrix of the finite element in the plastic range will change every moment with the change of stress state of the element.

The Stiffness Matrix of Triangular Elements

In the following, a division of the region into triangular shape elements is used. The simplest representation of the displacement increment of a node j of the triangular element is given by two linear polynomials.

$$\begin{aligned} \Delta u_j &= q_1 + q_2 x_j + q_3 y_j, \\ \Delta v_j &= q_4 + q_5 x_j + q_6 y_j, \end{aligned} \qquad (j = 1, 2, 3), \tag{6}$$

where

$\Delta u_j, \Delta v_j$: cartesian components of the displacement increment at a node j.

x_j, y_j: co-ordinate of a node j.

q_i $(i = 1, 2, 3, \ldots, 6)$: unknown quantity.

The alternative expression of eq. (6) is as follows,

$$\Delta \boldsymbol{\delta} = \boldsymbol{T}\boldsymbol{q}, \tag{7}$$

where

$$\Delta \boldsymbol{\delta} = \{\Delta u_1, \Delta u_2, \Delta u_3, \Delta v_1, \Delta v_2, \Delta v_3\},$$

$$\boldsymbol{q} = \{q_1, q_2, q_3, q_4, q_5, q_6\},$$

$$\boldsymbol{T} = \begin{bmatrix} 1 & x_1 & y_1 & 0 & 0 & 0 \\ 1 & x_2 & y_2 & 0 & 0 & 0 \\ 1 & x_3 & y_3 & 0 & 0 & 0 \\ 0 & 0 & 0 & 1 & x_1 & y_1 \\ 0 & 0 & 0 & 1 & x_2 & y_2 \\ 0 & 0 & 0 & 1 & x_3 & y_3 \end{bmatrix}.$$

The symbol {} means the transpose of the column vector.

The strain increment is defined in terms of the displacement increment.

$$\Delta \epsilon_x = \frac{\partial(\Delta u)}{\partial x}, \qquad \Delta \epsilon_y = \frac{\partial(\Delta v)}{\partial y}, \qquad \Delta \gamma_{xy} = \frac{\partial(\Delta u)}{\partial y} + \frac{\partial(\Delta v)}{\partial x}, \tag{8}$$

Which are written in matrix notation as,

$$\Delta \boldsymbol{\varepsilon} = \boldsymbol{B}\boldsymbol{q}, \tag{9}$$

where

$$\Delta \boldsymbol{\varepsilon} = \{\Delta \epsilon_x, \Delta \epsilon_y, \Delta \gamma_{xy}\},$$

$$\boldsymbol{B} = \begin{bmatrix} 0 & 1 & 0 & 0 & 0 & 0 \\ 0 & 0 & 0 & 0 & 0 & 1 \\ 0 & 0 & 1 & 0 & 1 & 0 \end{bmatrix}.$$

From eq. (7) and eq. (9),

$$\Delta \boldsymbol{\varepsilon} = \boldsymbol{B}\boldsymbol{T}^{-1}\Delta \boldsymbol{\delta}. \tag{10}$$

The relation between strain increment and stress increment is assumed to be linear during the increment.

$$\Delta \boldsymbol{\sigma} = \boldsymbol{D}^p \Delta \boldsymbol{\varepsilon}, \tag{11}$$

where $\Delta \boldsymbol{\sigma} = \{\Delta \sigma_x, \Delta \sigma_y, \Delta \tau_{xy}\}$,

$\boldsymbol{D}^p$: Elasto-plastic value of an elasticity matrix.

The increment of external work $\Delta \boldsymbol{E}$ done by nodal loads $\boldsymbol{F}$ is expressed as,

$$\Delta \boldsymbol{E} = -(\tfrac{1}{2}\Delta \boldsymbol{\delta}^* \Delta \boldsymbol{F} + \Delta \boldsymbol{\delta}^* \boldsymbol{F}), \tag{12}$$

where $*$: transpose of the matrix,

$\boldsymbol{F} = \{f_{1x}, f_{2x}, f_{3x}, f_{1y}, f_{2y}, f_{3y}\}$,

$\Delta \boldsymbol{F} = \{\Delta f_{1x}, \Delta f_{2x}, \Delta f_{3x}, \Delta f_{1y}, \Delta f_{2y}, 0 f_{3y}\}$,

$f_{ix}, f_{iy}\,(i = 1, 2, 3)$: components of external load at a node i,

$\Delta f_{ix}, \Delta f_{iy}\,(i = 1, 2, 3)$: components of load increment at a node i.

The corresponding increment of the strain energy $\Delta \boldsymbol{U}$ is,

$$\Delta \boldsymbol{U} = \int (\tfrac{1}{2}\Delta \boldsymbol{\varepsilon}^* \Delta \boldsymbol{\sigma} + \Delta \boldsymbol{\varepsilon}^* \boldsymbol{\sigma})\, dv. \tag{13}$$

From the principle of the minimum potential energy,

$$\Delta \boldsymbol{E} + \Delta \boldsymbol{U} = -(\tfrac{1}{2}\Delta \boldsymbol{\delta}^* \Delta \boldsymbol{F} + \Delta \boldsymbol{\delta}^* \boldsymbol{F}) + \int (\tfrac{1}{2}\Delta \boldsymbol{\varepsilon}^* \Delta \boldsymbol{\sigma} + \Delta \boldsymbol{\varepsilon}^* \boldsymbol{\sigma})\, dv = 0. \tag{14}$$

The next equation may be hold simultaneously, from the theorem of virtual work,

$$\int \Delta \boldsymbol{\varepsilon}^* \boldsymbol{\sigma}\, dv - \Delta \boldsymbol{\delta}^* \boldsymbol{F} = 0. \tag{15}$$

From eqs. (14) and (15),

$$\int (\tfrac{1}{2}\Delta \boldsymbol{\varepsilon}^* \Delta \boldsymbol{\sigma})\, dv - \tfrac{1}{2}\Delta \boldsymbol{\delta}^* \Delta \boldsymbol{F} = 0, \tag{16}$$

or

$$\Delta \boldsymbol{\varepsilon}^* \Delta \boldsymbol{\sigma} A t - \Delta \boldsymbol{\delta}^* \Delta \boldsymbol{F} = 0,$$

where A: area of the element,

t: thickness of the element,

Substituting eqs. (10) and (11), eq. (16) is written as,

$$\Delta \boldsymbol{F} = \boldsymbol{K}^p \Delta \boldsymbol{\delta}, \tag{17}$$

where $$\boldsymbol{K}^p = \boldsymbol{N}^* \boldsymbol{D}^p \boldsymbol{N} A t, \qquad \boldsymbol{N} = \boldsymbol{B}\boldsymbol{T}^{-1}.$$

Elastic-Plastic Value of an Elasticity Matrix of the Material

After POPE [2], the elasticity matrix in inelastic range $\boldsymbol{D}^p$ is derived as follows:

The yield condition may be represented by a yield surface which is given by

$$f(\sigma_{ij}) = 0, \tag{18}$$

where σ_{ij} is a nine component stress tensor. It should be noted, however, that the stress tensor is symmetrical and that consequently only six of the stress components are independent.

If it is assumed that changes in the yield surface during deformation depend on plastic strain history only, the yield condition after a further infinitesimal increment of plastic strain is given by

$$f + t_{ij}\, d\epsilon_{ij}^p + \frac{\partial f}{\partial \sigma_{ij}} d\sigma_{ij} = 0.$$

Hence $$t_{ij}\, d\epsilon_{ij}^p = -\frac{\partial f}{\partial \sigma_{ij}} d\sigma_{ij}, \tag{19}$$

where t_{ij} describes the strain-hardening properties.

The plastic strain increments are given by

$$d\epsilon_{ij}^p = \lambda \frac{\partial f}{\partial \sigma_{ij}}, \tag{20}$$

where λ is the plastic strain increment factor.

We denote by the suffix 0 symbols relating to some initial loaded state in which the stresses and strains are known in a typical triangular element. The total strains after this initial state has been modified by a small load increment is given by

$$\boldsymbol{\varepsilon} = \boldsymbol{\varepsilon}_0 + \delta \boldsymbol{\varepsilon}^e + \delta \boldsymbol{\varepsilon}^p, \tag{21}$$

where $$\boldsymbol{\varepsilon} = \{\epsilon_{11}, \epsilon_{22}, 2\epsilon_{12}, \epsilon_{33}\} \tag{22}$$

and where $\delta \epsilon^e$ and $\delta \epsilon^p$ are corresponding matrices of the elastic and plastic strain increments.

Provided that there is no significant change in the elastic constants during the load increments, the elastic strain increments are given by

$$\boldsymbol{\sigma} - \boldsymbol{\sigma}_0 = \boldsymbol{D}_0^e \delta \boldsymbol{\varepsilon}^e, \tag{23}$$

where $$\boldsymbol{\sigma}_0 = \{\sigma_{11}, \sigma_{22}, \sigma_{12}, \sigma_{33}\}, \tag{24}$$

and where $\boldsymbol{D}_0^e$ is the elasticity matrix.

Eq. (20) is expressed approximately by a matrix form

$$\delta \boldsymbol{\varepsilon}^p = \lambda \boldsymbol{\Phi}_0, \tag{25}$$

where

$$\boldsymbol{\Phi} = \left\{\frac{\partial f}{\partial \sigma_{11}}, \frac{\partial f}{\partial \sigma_{22}}, 2\frac{\partial f}{\partial \sigma_{12}}, \frac{\partial f}{\partial \sigma_{33}}\right\}. \tag{26}$$

When yielding is governed by the von Mises criterion, eq. (26) is written

$$\boldsymbol{\Phi} = \{\sigma'_{11}, \sigma'_{22}, \sigma'_{12}, \sigma'_{33}\},$$

where superscript $'$ denotes the deviatric stress.

Provided that the stress increments are small compared with the stresses themselves, the following linearized form of eq. (19) may be used.

$$\boldsymbol{\Psi}\, \delta \boldsymbol{\varepsilon}^p = -\boldsymbol{\Phi}_0^* (\boldsymbol{\sigma} - \boldsymbol{\sigma}_0), \tag{27}$$

where

$$\boldsymbol{\Psi} = [t_{11}, t_{22}, t_{12}, t_{33}]. \tag{28}$$

Substituting eq. (21) and (25) in eq. (23), it may be shown that

$$\boldsymbol{\sigma} - \boldsymbol{\sigma}_0 = \boldsymbol{D}_0^e (\boldsymbol{\varepsilon} - \boldsymbol{\varepsilon}_0 - \lambda \boldsymbol{\Phi}_0). \tag{29}$$

λ may be obtained by substituting eq. (25) and (29) in eq. (27)

$$\lambda = L\, \boldsymbol{\Phi}_0^*\, \boldsymbol{D}_0^e (\boldsymbol{\varepsilon} - \boldsymbol{\varepsilon}_0), \tag{30}$$

where L is a scalar given by

$$L^{-1} = \boldsymbol{\Phi}_0^*\, \boldsymbol{D}_0^e\, \boldsymbol{\Phi}_0 - \boldsymbol{\Psi}_0\, \boldsymbol{\Phi}_0. \tag{31}$$

Substituting eq. (30) in eq. (29)

$$\boldsymbol{\sigma} - \boldsymbol{\sigma}_0 = \boldsymbol{D}_0^e (\boldsymbol{I} - L\, \boldsymbol{\Phi}_0\, \boldsymbol{\Phi}_0^*\, \boldsymbol{D}_0^e)(\boldsymbol{\varepsilon} - \boldsymbol{\varepsilon}_0). \tag{32}$$

Hence

$$\begin{aligned} \boldsymbol{\sigma} - \boldsymbol{\sigma}_0 &= \boldsymbol{D}^p (\boldsymbol{\varepsilon} - \boldsymbol{\varepsilon}_0), \\ \boldsymbol{D}^p &= \boldsymbol{D}_0^e (\boldsymbol{I} - L\, \boldsymbol{\Phi}_0\, \boldsymbol{\Phi}_0^*\, \boldsymbol{D}_0^e), \end{aligned} \tag{33}$$

where $\boldsymbol{I}$ denotes a unit diagonal matrix and where $\boldsymbol{D}^p$ is the elastic-plastic value of an elasticity matrix.

When the element is in a state of plane stress, the $\boldsymbol{D}_0^e$ matrix is written in the form

$$\boldsymbol{D}_0^e = \frac{E}{1-\nu^2} \begin{bmatrix} 1 & \nu & 0 & 0 \\ \nu & 1 & 0 & 0 \\ 0 & 0 & \frac{1-\nu}{2} & 0 \\ 0 & 0 & 0 & 0 \end{bmatrix}. \tag{34}$$

Using this expression, $\boldsymbol{D}^p$ of eq. (33) is calculated as follows,

$$\boldsymbol{D}^p = \frac{E}{C_2}\begin{bmatrix} \sigma_y'^2 + 2C_1 & -\sigma_x'\sigma_y' + 2\nu C_1 & -\dfrac{\sigma_x' + \nu\sigma_y'}{1+\nu}\tau_{xy} \\ & \sigma_x'^2 + 2C_1 & -\dfrac{\sigma_y' + \nu\sigma_x'}{1+\nu}\tau_{xy} \\ \text{(symmetric)} & & C_3 \end{bmatrix}, \tag{35}$$

where $C_1 = \dfrac{2H'}{9E}\bar{\sigma}^2 + \dfrac{\tau_{xy}^2}{1+\nu}$,

$C_2 = \sigma_x'^2 + 2\nu\sigma_x'\sigma_y' + \sigma_y'^2 + 2(1-\nu^2)C_1$,

$C_3 = \dfrac{1}{2(1+\nu)}\{\sigma_x'^2 + 2\nu\sigma_x'\sigma_y' + \sigma_y'^2\} + \dfrac{2H'}{9E}(1-\nu)\bar{\sigma}^2$,

$\left.\begin{aligned}\sigma_x' &= \tfrac{1}{3}(2\sigma_x - \sigma_y)\\ \sigma_y' &= \tfrac{1}{3}(2\sigma_y - \sigma_x)\end{aligned}\right\}$ deviatric stress,

E: Young's modulus,

ν: Poisson's ratio,

$\bar{\sigma}^2 = \sigma_x^2 + \sigma_y^2 - \sigma_x\sigma_y + 3\tau_{xy}^2$,

$H' = \dfrac{\Delta\bar{\sigma}}{\Delta\bar{\epsilon}^p}$,

$\Delta\bar{\epsilon}^p = \dfrac{2\bar{\sigma}}{3C_2}[(\sigma_x' + \nu\sigma_y')\Delta\epsilon_x + (\sigma_y' + \nu\sigma_x')\Delta\epsilon_y + (1-\nu)\tau_{xy}\Delta\gamma_{xy}]$

equivalent plastic strain increment.

The expression of eq. (35) coincides with that appeared in the later contribution of Y. YAMADA [3].

The strain increment in the direction of the thickness $\Delta\epsilon_z$ is obtained from the assumption that the plastic deformation may occur with no volume change,

$$\Delta\epsilon_z = -\Delta\epsilon_x - \Delta\epsilon_y + \frac{(1-2\nu)}{E}(\Delta\sigma_x + \Delta\sigma_y). \tag{36}$$

Determination of the Load Increment

The stiffness matrices of respective triangular elements eq. (17) are assembled to that of whole structural system now considering, then $\Delta\boldsymbol{F}$ represents the increment of the applied load. $\Delta\boldsymbol{\delta}$, $\Delta\boldsymbol{\varepsilon}$ and $\Delta\boldsymbol{\sigma}$ may be obtained for the given value of $\Delta\boldsymbol{F}$ from eq. (17), eq. (10) and eq. (11) respectively.

Stress-strain relation of the steel is characterized by yield point and strain-hardening point, and to study the inelastic behavior of steel specimen, it is important to check the status corresponding to these points. This is performed by the following procedure,

1. The distribution of the applied forces $\boldsymbol{F}$ or $\Delta \boldsymbol{F}$ are indicated by their ratios.
2. An arbitary value of $\Delta \boldsymbol{F}$ is given according to their distribution, and $\Delta \boldsymbol{\sigma}$, $\Delta \boldsymbol{\varepsilon}$ of each triangular element are calculated.
3. It is necessary to apply the load $m \Delta \boldsymbol{F}$ to make yield an arbitrary triangular element, the condition for this may be expressed as follows,

$$\sigma_Y = (\sigma_x + m \Delta \sigma_x)^2 + (\sigma_y + m \Delta \sigma_y)^2 - (\sigma_x + m \Delta \sigma_x)(\sigma_y + m \Delta \sigma_y) + 3(\tau_{xy} + m \Delta \tau_{xy})^2, \tag{37}$$

where, m: multiplying factor.

Calculate the values of m for all triangular elements, and the minimum value of them is the necessary multiplying factor to produce the first yield of any triangular elements.

4. Determine the value of m which make yield the next triangular elements by the similar procedure as described above, in this step however, it must be considered whether the strain of the already yielded element should reach the strain hardening point or not by the increment of the load $m \Delta \boldsymbol{F}$. This condition may be expressed as,

$$m \Delta \bar{\epsilon}^p = \epsilon_{st} - \sum \Delta \bar{\epsilon}^p. \tag{38}$$

Then in this step, eq. (37) and eq. (38) must be considered simultaneously to determine the minimum value of m.

5. In successive calculations, co-ordinates of nodes and thickness of the elements must be based upon the state just before the each load increment should be given.

Appendix II. Notation

The following symbols are used in this paper:

A	=	area of the element
$A(0)$	=	minimum sectional area of the specimen
$A(x)$	=	sectional area at x
A_{min}	=	minimum sectional area of the member
A_p	=	sectional area of the parallel part of the member
$\boldsymbol{B}$	=	matrix defined by eq. (9)
C_1, C_2, C_3	=	functions defined by eq. (35)
$\boldsymbol{D}_0^e$	=	elasticity matrix
$\boldsymbol{D}^p$	=	elastic-plastic value of an elasticity matrix
E	=	Young's modulus
$\Delta \boldsymbol{E}$	=	increment of the external work

$\boldsymbol{F}$	=	nodal load vector
$\Delta \boldsymbol{F}$	=	increment of the nodal load vector
f_{ix}, f_{iy}	=	Cartesian components of external load at a node i
$\Delta f_{ix}, \Delta f_{iy}$	=	Cartesian components of load increment at a node i
H'	=	strain hardening modulus
$\boldsymbol{I}$	=	unit diagonal matrix
K	=	load step
$\boldsymbol{K}^p$	=	stiffness matrix of a triangular element in inelastic range
L	=	half length of the specimen or a scalar given by eq. (31)
m	=	multiplying factor
$\boldsymbol{N}$	=	matrix defined by eq. (17)
$\boldsymbol{q}$	=	unknown vector
q	=	unknown quantity
$\boldsymbol{T}$	=	matrix defined by eq. (7)
T	=	tensile load
t	=	thickness of the element
t_{ij}	=	strain-hardening properties
T_{max}	=	maximum tensile load of the specimen
$\Delta \boldsymbol{U}$	=	increment of the strain energy
$\Delta u_j, \Delta v_j$	=	Cartesian components of displacement increment at *a* node j
V_i	=	volume of a triangular element i
X	=	length of the yielded zone
Y	=	yield ratio of the material
α	=	load index
δ_L	=	elongation of the half length of the specimen
δ_{max}	=	elongation of the half length of the specimen at the maximum load
$\delta_{GG'}$	=	elongation of the specimen between G and G' (Fig. 4, 8)
$\delta_{BB'}$	=	elongation of the specimen between B and B' (Fig. 12)
$\Delta \boldsymbol{\delta}$	=	increment of displacement vector
$\Delta \boldsymbol{\varepsilon}$	=	$\{\Delta \epsilon_x, \Delta \epsilon_y, \Delta \gamma_{xy}\}$ = increment of strain vector
$\bar{\epsilon}$	=	average strain
ϵ_Y	=	strain at yield point
ϵ_B	=	strain at tensile strength point
ϵ_{st}	=	strain at the start of strain hardening
$\Delta \bar{\epsilon}^p$	=	increment of the equivalent strain
$\delta \boldsymbol{\varepsilon}^e$	=	elastic strain increment
$\delta \boldsymbol{\varepsilon}^p$	=	plastic strain increment
$\sum \Delta \bar{\epsilon}^p$	=	equivalent strain
λ	=	plastic strain increment factor
ν	=	Poisson's ratio
$\bar{\sigma}$	=	equivalent stress
σ_B	=	tensile strength

$\sigma(x)$ = average stress at x
σ_Y = yield point
$\sigma_{AA'}$ = average stress at A–A' section
$\boldsymbol{\sigma}$ = stress vector
$\Delta\boldsymbol{\sigma}$ = increment of stress vector
σ' = deviatric stress
σ_{ij} = nine component stress tensor
$\boldsymbol{\Phi}$ = see eq. (26)
$\boldsymbol{\Psi}$ = see eq. (28)

Appendix III. References

1. Lay, M. G., and Smith, P. D., Role of Strain hardening in Plastic Design, Journal of the Structural Division, Proc. of the A.S.C.E., June 1965.
2. Pope, G. G., The Application of the Matrix Displacement Method in Plane Elasto-Plastic Problems, Proc. of the Conference held at Wright-Patterson Air Force Base, Ohio, Oct. 1965.
3. Y. Yamada et al., Plastic Stress-Strain Matrix and its Application for the Solution of Elastic-Plastic Problems by the Finite Element Method, International Journal of Mechanical Sciences. Vol. 10, No. 5. May 1968.

Summary

Deformation capacity of steel tension members of which sectional area change continuously along their length is investigated analytically and experimentally. When the change of the sectional area along the length is gradual, the stress concentration is negligible, on the contrary, when the change is very steep as in the case of bolt-hole, the effect of the stress concentration can not be ignored. For the analysis of the latter case, the finite element method extended to the elastic-plastic range based on the plastic flow theory is adopted. The agreement of the theory with the test result is satisfactory.

Résumé

On étude théoriquement et expérimentalement l'aptitude à la déformation de pièces d'acier soumises à des efforts et dont la section varie longitudinalement. Si la variation de section est progressive longitudinalement, la concentration des efforts est négligeable. Au contraire, si la variation est brusque comme dans le cas d'un alésage pour boulon, l'effet de la concentration des efforts ne peut être ignoré. Dans l'analyse de ce dernier cas, on adopte la

méthode considérant des éléments finis étendue au domaine élastique-plastique et basée sur la théorie du fluage. Les mesures expérimentales concordent de manière satisfaisante avec les résultats théoriques.

Zusammenfassung

Analytisch und experimentell ist die Verformungsfähigkeit von Stahlelementen untersucht worden, deren Querschnitte kontinuierlich ändern. Ist die Querschnittsänderung allmählich, so kann die Spannungskonzentration vernachlässigt werden, ist die Änderung jedoch schroff wie im Falle eines Nietloches, dann kann sie nicht vernachlässigt werden. Für die Berechnung des letzteren Falles wurde die für den elastisch-plastischen Bereich auf Grund der Fließtheorie erweiterte Endlichen-Elementen-Methode angewandt. Die Übereinstimmung der Theorie mit den Versuchsergebnissen ist zufriedenstellend.